

Fuzzy geometric feature-based texture classification

P. Kundu and B.B. Chaudhuri

Electronics and Communication Sciences Unit, Indian Statistical Institute, 203 B.T. Road, Calcutta 700 035, India

Abstract

Kundu, P. and B.B. Chaudhuri, Fuzzy geometric feature-based texture classification, Pattern Recognition Letters 14 (1993) 825–832.

It is necessary to compute various spatial and gray-level properties for the classification of textured regions of an image. However, the regions and their properties are not always crisply defined. It is more appropriate to regard them as fuzzy subsets of the image. In this paper we have proposed the use of fuzzy geometric properties for texture classification. At first, a set of 2-D local membership-value extrema have been detected on the image. Using them as 'seed' regions, they are grown till the grown regions do not touch any other seed regions. The resulting regions are called the regions of influence. Fuzzy geometric properties like fuzzy area, perimeter, compactness, height and width are determined on these regions and they constitute the feature space for texture classification. Several natural textures are digitized and used to test the efficiency of the approach. It is seen that about 90% classification accuracy is obtained in the pattern space of 8 textures.

Keywords. Fuzzy sets, fuzzy geometry, texture analysis, classification, image processing.

1. Introduction

Texture plays an important role in classification and segmentation of pictures in computer vision and image analysis problems. Texture is a region property and can be characterized roughly as a field consisting of typical microstructures. An important characteristic of texture is its dependence on spatial resolution. Haralick [7] has pointed out that tone (i.e., gray level) and texture are both present in the image at the same time, but depending on circumstances one or

other may dominate. When there is a large variation in the tonal primitives in a relatively small area of an image, texture becomes the dominant property. However, to classify an image into several textured regions, we need to compute various properties of and relationships among these regions. For a natural texture image these regions and their properties are not always *crisply* defined. It is more appropriate to regard them as fuzzy subsets of the image. Rosenfeld [11,12] extended many standard geometric properties of and relations among regions to gray-tone image space using the framework of fuzzy set theory and called this extension the *fuzzy geometry* of image space. The generalization includes the concept of connectedness, surroundedness, adjacency, convexity, area, perimeter, compactness, height, width,

Correspondence to: Prof. B.B. Chaudhuri, Electronics and Communication Sciences Unit, Indian Statistical Institute, 203 B.T. Road, Calcutta 700 035, India. Email: ncst.ernet.in!kbcsca!bbc

elongatedness etc. Chaudhuri [3,4] gave some shape definitions in fuzzy geometry, e.g. circle, ellipse, polygon etc. He also introduced the concept of concave fuzzy set and established its properties in the context of fuzzy geometry. In this paper we have used fuzzy geometric properties to classify different textures in an image.

It has been established that useful texture properties can be found from 1-D local extrema. See, for example, Rosenfeld and Troy [13], Ledley [8], Rotolo [14], Mitchell et al. [9]. In this paper we have considered 2-D local extrema regions and used them to find the regions which may capture the perceived variation in tonal primitives.

Going beyond the simple counting of local extrema, we have associated fuzzy geometric properties to the regions originated from each extremum. For example, given a local maximum, we can determine the set of all pels reachable only by the given local maximum and not by any other local maxima by a path of monotonically non-increasing membership values. This set of reachable pels is defined as a connected region. It can be viewed as a hill whose border pels may be local minima or saddle pels. We have used fuzzy geometric properties such as area, perimeter, compactness, etc. on these regions and used them as texture features for classification.

Section 2 contains a brief discussion of fuzzy set concepts in image processing. Some definitions of fuzzy geometry are given in Section 3. Detection of 2-D local extrema has been discussed in Section 4. Texture features are derived in Section 5 while the classification results are presented in Section 6.

2. Fuzzy set concept in image processing

Prewitt [10] first noticed the possibility of using fuzzy set concepts in image processing. According to the Gestalt principles, there exist two distinguishable aspects in an image namely *background* and *object*. However, the background/object demarcation in a gray-tone image is not easy, especially in automatic digital image processing. Fuzzy set offers a conceptual framework to describe an object in such a situation.

Let the object be considered as a fuzzy set, so that each pel p in the image has a membership $0 \leq \mu(p) \leq 1$

of being a *constituent part* of the object. Note that we use the phrase *constituent part* instead of the word *member*. To see the distinction, consider the membership of a person belonging to the fuzzy set 'young person' as compared to the membership of a 'limb' belonging to the concept 'body'. In the former case the membership identifies the person with the concept 'young person' while in the latter case the membership identifies the 'limb' as the constituent part of the 'body'.

The simplest way to represent the image as a fuzzy set is by normalizing the gray levels. Thus, if a pel p has gray level $f(p)$ then we can define a fuzzy set μ so that $\mu(p) = f(p)/255$. Clearly, $0 \leq \mu \leq 1$. The definition of μ can be slightly modified for an image having minimum and maximum gray levels f_{\min} and f_{\max} as

$$\mu(p) = \frac{f(p) - f_{\min}}{f_{\max} - f_{\min}}. \quad (1)$$

Note that still $0 \leq \mu \leq 1$, and μ is monotonic and linear on gray levels. To make it nonlinear, a power $\beta \neq 1$ on the right-hand side of the above equation may be used.

We have used equation (1) to define the fuzzy membership. It should be cautioned that the membership assignment is a nontrivial problem. Some discussion on the topic is available in Chaudhuri [6].

3. Fuzzy geometric properties

A fuzzy subset of a set S is a mapping μ from S into $[0,1]$. For any $P \in S$, $\mu(P)$ is called the degree of membership of P in μ . A crisp (i.e., ordinary, non-fuzzy) subset of S can be regarded as a special case of fuzzy subset, where the mapping μ is into $\{0, 1\}$. S is called the support set of μ . The level sets of μ are the sets

$$\mu_t = \{P \in S \mid \mu(P) \geq t\}, \quad 0 \leq t \leq 1.$$

We consider digital fuzzy sets as special cases of *piecewise constant* fuzzy sets having constant value on each of a finite set of bounded regions that meet pairwise along rectifiable arcs. A discrete fuzzy subset can be defined on each of the connected components of the image. Here, each pel of the component belongs to the support set of the fuzzy subset.

Some existing properties [12]

1. *Area.* The area of a fuzzy subset μ is defined as

$$a(\mu) = \int \mu \, dx \, dy$$

where the integration is taken over a region outside which $\mu=0$.

In case of a discrete fuzzy subset μ on image space with support C , where μ is piecewise constant, the area becomes

$$a(\mu) = \sum_{(x,y) \in C} \mu(x,y) .$$

2. *Perimeter.* If μ is piecewise constant let μ_i and μ_j be two constant values of membership where the two regions meet. The perimeter of μ is defined as

$$p(\mu) = \sum_{i,j,k,i < j} |\mu_i - \mu_j| \cdot |A_{ijk}| .$$

This is just the weighted sum of the lengths of the arcs A_{ijk} along which the regions on which μ has constant value meet, weighted by the absolute differences of these values.

3. *Compactness.* The compactness of a fuzzy subset μ is defined as

$$c(\mu) = a(\mu) / p^2(\mu)$$

where $a(\mu)$ and $p(\mu)$ are the area and perimeter of μ , respectively. For crisp sets, the compactness is maximum for a disc, where it is equal to $1/4\pi$. In case of a fuzzy disc, where the membership value μ depends only on the distance from the center, this compactness measure satisfies $c(\mu) \geq 1/4\pi$. Thus, of all possible fuzzy discs, the compactness is smallest for its crisp version.

4. *Height and width.* The height and width of a fuzzy subset μ are defined, respectively, as

$$h(\mu) = \int \left[\max_x \{ \mu(x,y) \} \right] dy \quad \text{and}$$

$$w(\mu) = \int \left[\max_y \{ \mu(x,y) \} \right] dx .$$

4. Extrema detection

For the detection of 2-D maximally connected extrema we have used the method (EXTREMA-1) proposed by Chaudhuri and Uma Shankar [5]. The extrema components of an image are defined as follows.

Let S denote the set of pels of an image. Let R be an 8-connected component in S . If \bar{R} is the component of R in S , then the border of \bar{R} with R is defined as the subset $B(\bar{R}, R)$ of R , any element of which is the 8-neighbor of at least one element of R . A component R in S is a local maximum or more generally, a plateau in S if the membership values of all elements in R are equal and this value is greater than the membership value of any element in $B(\bar{R}, R)$. Similarly, R is a local minimum or valley in S if the membership values of pels in R are equal but less than the membership value of any element in $B(\bar{R}, R)$.

The idea behind the algorithm EXTREMA-1 of [6] is to find pels that are not extrema, and to find connected components of the same membership value and delete them. Here the pels are considered in a row scanning manner. First, each candidate pel (CAP) is labelled as either (a) an extremum or (b) neither a minimum or maximum in its 3×3 neighborhood. When (b) is true, the CAP is called a collapsible pel (CP). Examples of these cases are shown below.

0.2	0.4	0.8	0.4	0.2	0.3
0.3	<u>0.8</u>	0.7	0.6	<u>0.2</u>	0.3
0.6	0.6	0.6	0.5	0.4	0.2

Maximum Minimum

0.2	0.4	0.8
0.4	<u>0.8</u>	0.7
0.7	0.7	0.9

Collapsible pel (CP)

If a CP is encountered, its connected component of pels of the same membership value is found and all pels belonging to this component are collapsed. The result is stored in a matrix whose dimensions are the same as that of the original image matrix. The collapsed pels are labelled by, say, -1 in the corresponding positions of the result matrix while the extrema are labelled by, say, 1. The result matrix is ini-

tially empty, i.e., all entries are labelled as 0.

In actual implementation, for each CAP, the corresponding position in the result matrix is examined if the label there is -1 , i.e., if it is already collapsed by any previous CP. In case the CAP is already collapsed, no test of maximum or minimum is made. In case the CAP is not collapsed and it is found to be a CP, its corresponding connected component is found and collapsed; otherwise, it is considered as an extremum. All results corresponding to the current CAP are stored in the result matrix.

5. Feature evaluation

The extrema components are found using the method described in Section 4. We associate geometrical properties to the regions grown from these local extrema. We describe here the growth process starting from the maxima components. The growth process starting from the minima components can be understood in a similar manner.

Suppose M is a local maximum and (i, j) is a pel in it. We determine the set of all pels reachable only from (i, j) and not from the pels of other local maxima by monotonically non-increasing paths. (If P and Q are two pixels then a *non-increasing path* between P and Q is a sequence $P=p_0, p_1, \dots, p_n=Q$ so that p_i is the neighbor of p_{i-1} and their membership values satisfy the inequality $\mu(p_i) \geq \mu(p_{i+1})$, $i=0, 1, \dots, n-1$.) These reachable pels are kept in a stack denoted by \mathcal{S}_M . Initially \mathcal{S}_M contains only the (i, j) th pel. We check all the 8-neighbors of each member of the stack to see whether any of them is either a maximum or a minimum. If an 8-neighbor of the members of the stack is an extremum (other than M) then these neighboring pels are pushed into the stack \mathcal{S}_M . In this way the stack \mathcal{S}_M is grown until one of the 8-neighbors of at least one of its members is an extremum pel not belonging to M . Note that for any M , \mathcal{S}_M contains at least 9 elements. This process of growing the stack is done for all the maxima of the image.

Let \mathcal{S} be the set of stacks corresponding to all maxima of the given image. In terms of the membership values each stack of \mathcal{S} forms a hill whose border may be local minima or saddle points. The space of this region may be called the *region of influence (RI)*. The size of this region is the number of pels in the corre-

sponding stack. The set of stacks \mathcal{S} can be treated as the set of regions which corresponds to the perceived variation in the tonal primitives. If the size of the regions of \mathcal{S} are small, it is expected that the image is busy so that the variation in the tonal primitives is high. Geometric shapes and relations of these regions are thus important cues to characterize the texture present in the image.

Without loss of generality, we denote the *RI* originated from the maximum M by \mathcal{S}_M . For every *RI* \mathcal{S}_M of \mathcal{S} we find the size \mathcal{A}_M of the *RI* by counting the number of its elements. To describe \mathcal{S}_M geometrically, we use the measures defined in Section 3.

If \mathcal{A}_M denotes the area of \mathcal{S}_M then

$$\mathcal{A}_M = \sum_{l,m \in \mathcal{S}_M} \mu_{l,m}$$

where $\mu_{l,m}$ denotes the membership value of the (l, m) th pel and the summation is taken over all the elements of \mathcal{S}_M .

The *perimeter* \mathcal{P}_M of \mathcal{S}_M is obtained by considering each element of \mathcal{S}_M and its four neighbors, each of which belongs to \mathcal{S}_M :

$$\mathcal{P}_M = \frac{1}{2} \{ |\mu_{l,m} - \mu_{l,m-1}| + |\mu_{l,m} - \mu_{l,m+1}| + |\mu_{l,m} - \mu_{l-1,m}| + |\mu_{l,m} - \mu_{l+1,m}| \}$$

The *compactness* \mathcal{C}_M of \mathcal{S}_M is

$$\mathcal{C}_M = \mathcal{A}_M / \mathcal{P}_M$$

The *height* \mathcal{H}_M and *width* \mathcal{W}_M of \mathcal{S}_M are, respectively,

$$\mathcal{H}_M = \sum_l \max \mu_{l,m} \quad \text{and} \quad \mathcal{W}_M = \sum_m \max \mu_{l,m}$$

where the summations are taken over all elements of \mathcal{S}_M .

It has been noted that \mathcal{S}_M contains pels reachable only by M and they form a 'hill' whose border pels are either local minima or saddle points. In addition to the above measures, we also consider the relative height of this hill. If there exist more than one minimum on the border then we choose the highest of these minima and call it m_{ij} . In case of only one minimum on the border, we call that minimum m_{ij} . The *relative height* H_M of the 'hill' is taken as

$$H_M = |\mu_M - \mu_{m_{ij}}|$$

where μ_M and $\mu_{m_{ij}}$ are the membership values of the pels corresponding to M and m_{ij} , respectively.

In a similar manner, the above measures are found for all regions of influence of \mathcal{A} . Now, let the size of the image be $N \times N$. The total area of the image is then

$$\mathcal{A} = \sum_{(i,j) \in N \times N} \mu_{i,j}$$

where $\mu_{i,j}$ denotes the membership value of the (i, j) th pel. Also let \mathcal{E} denote the total number of extrema of the given image. The normalized features of an image are defined as follows.

$$f_1 = \mathcal{E} / \mathcal{A}, \tag{2}$$

$$f_2 = (\sum_M \mathcal{A}_M) / \mathcal{A}, \tag{3}$$

$$f_3 = (\sum_M \mathcal{P}_M) / \mathcal{A}, \tag{4}$$

$$f_4 = (\sum_M \mathcal{C}_M) / \mathcal{A}, \tag{5}$$

$$f_5 = (\sum_M H_M) / \mathcal{A}, \tag{6}$$

$$f_6 = (\sum_M V_M) / \mathcal{A}, \tag{7}$$

$$f_7 = (\sum_M \#_M) / \mathcal{A}, \tag{8}$$

$$f_8 = (\sum_M \#_M) / \mathcal{A}. \tag{9}$$

6. Classification results and discussion

A set of 16 texture images from the Brodatz album [1] are used for testing the efficiency of the proposed method. The images are digitized in 128×128 pels with 0–255 quantized gray levels. The textures are shown in Figure 1, where both oriented and non-ori-

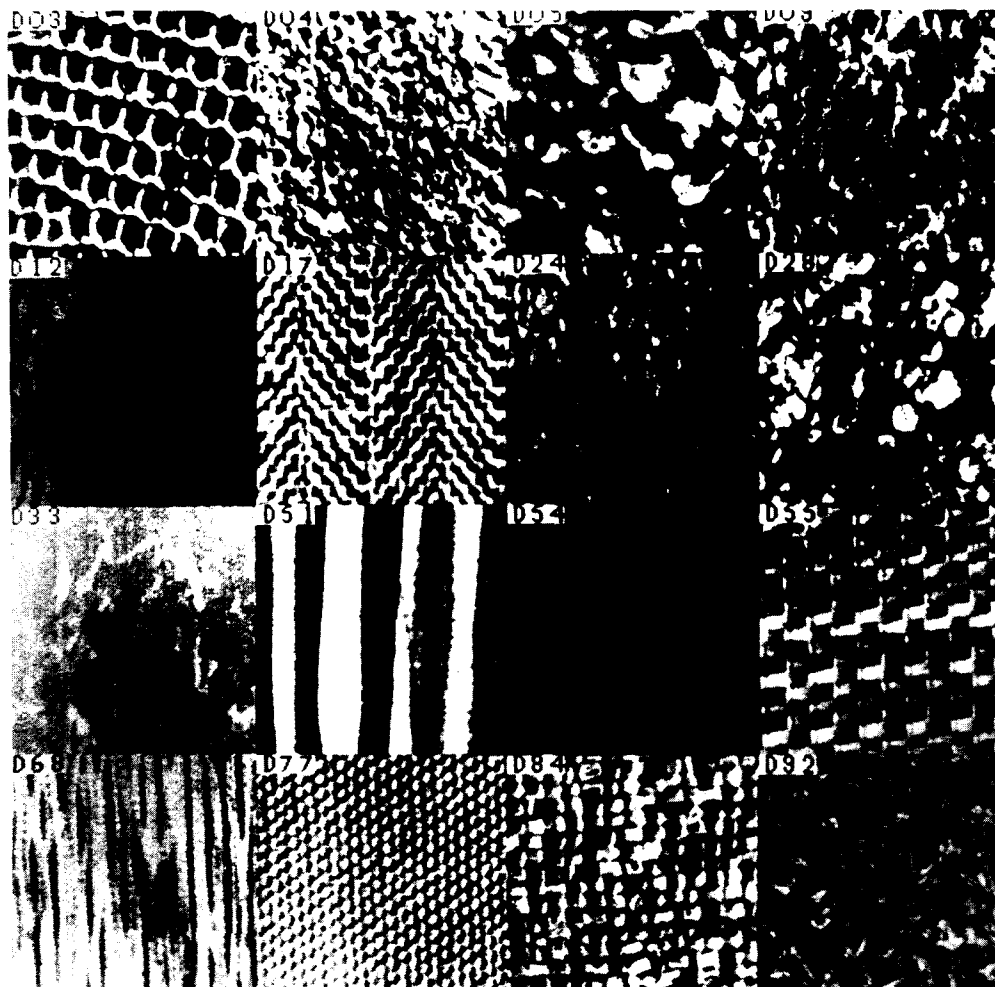


Figure 1. 16 texture mosaics from Brodatz's album [1].

ented textures of different types are presented.

Computation of any feature at a pel is done on a window of size 32×32 pels around that pel. The pels are chosen randomly during training as well as during classification experiments. On each of these pels, at first the extrema are located on its 32×32 neighborhood using the algorithm in Section 4 and then the region of influence of each extremum is computed using the procedure in Section 5. All the eight features f_1-f_8 are computed at each pel using equations (2)-(9). Thus, the pattern is represented in an 8-dimensional feature space. Figure 2 represents the histograms of the normalized feature values of the image D17. From the histograms it is clear that the features are well clustered for a texture image. Similar results can be obtained with other features as well.

The classifier is trained using samples of different size for which the class status is assumed known. The mean vector m_i and the standard deviation vector σ_i of training samples for each class are found. Each

mean vector represents the seed point of the corresponding class. During the classification phase, the weighted distance of an unknown sample is computed from the seed point by weighting the Euclidean distance by the corresponding standard deviation components. In other words, if the sample vector is x_k , then its distance from the i th seed point is

$$d_i = \left\{ \frac{\sum_{j=1}^8 \|x_{kj} - m_{ij}\|^2}{\sigma_{ij}^2} \right\}^{1/2}$$

x_k is assigned to the class i if d_i is minimum over all i .

Table 1 shows the classification matrix for our method using 100 test samples and 30 training samples. It is clear that maximum confusion occurs between the textures D09 and D84. Visually too, these two textures have somewhat identical grain size.

Plots of the classification rate against the number of texture classes considering 100 test samples are

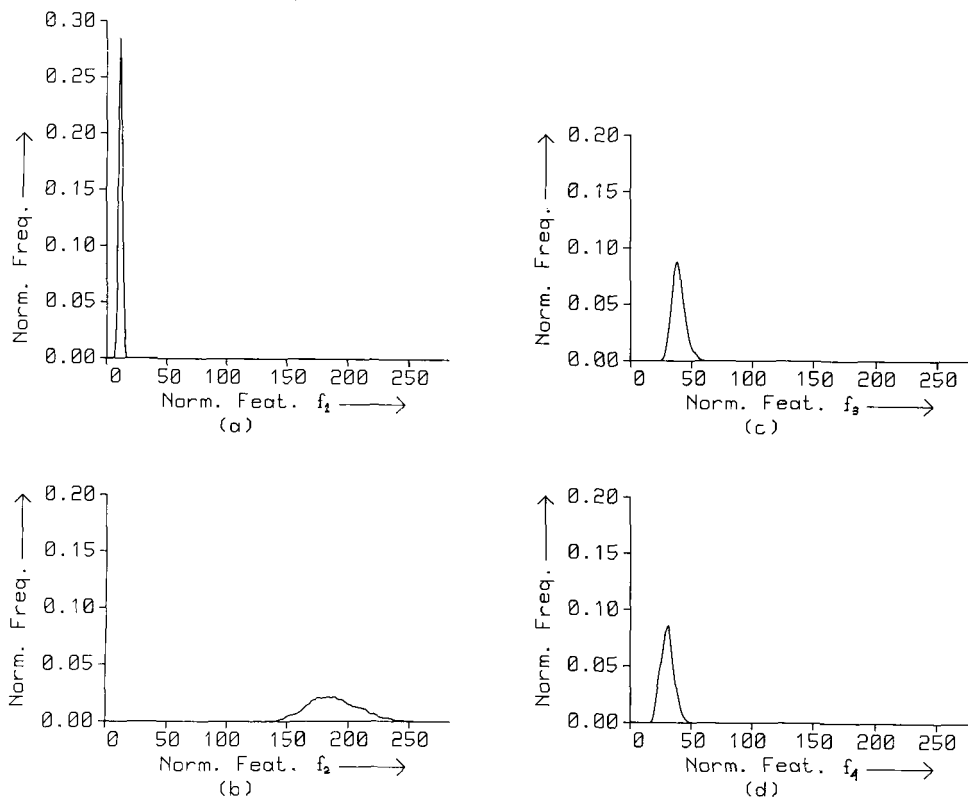


Figure 2. Feature value histograms for a texture image.

Table 1
Confusion matrix of texture classification

	D09	D12	D05	D84	D68	D55	D77	D51
D09	68	0	0	32	0	0	0	0
D12	0	100	0	0	0	0	0	0
D05	0	0	80	0	0	14	0	6
D84	2	0	0	96	0	2	0	0
D68	0	0	0	0	91	4	0	5
D55	0	0	0	0	1	98	0	1
D77	0	0	0	0	0	0	100	0
D51	0	0	0	0	0	0	0	100

given in Figure 3 where (a) and (b) represent the classification curve using 10 and 30 training samples, respectively. It is seen from the plots that the classification rate increases with an increase in the number of training samples. The experiment has been re-

peated using 50, 150 and 200 test samples. In all cases, the shape of the results is similar, except that the classification error increases slowly with the number of

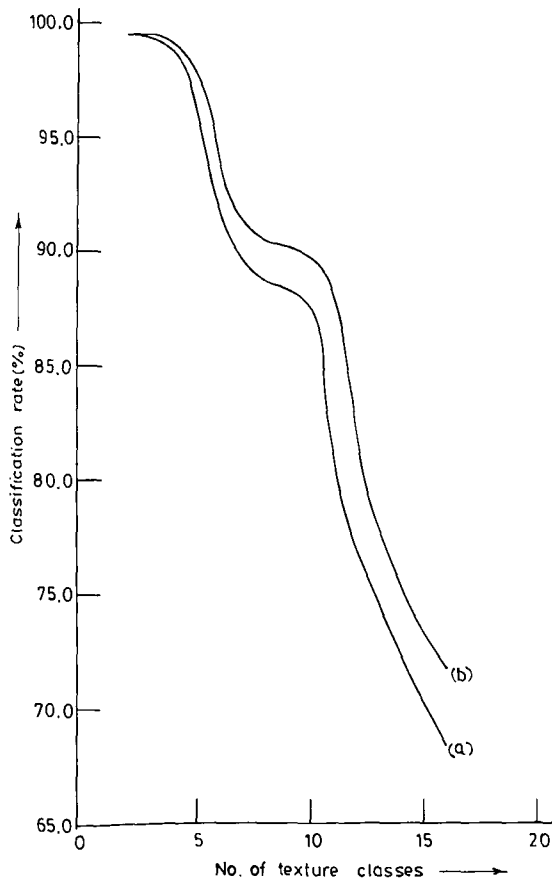


Figure 3. Classification rate of 100 test samples: (a) using 10 training samples, (b) using 30 training samples.

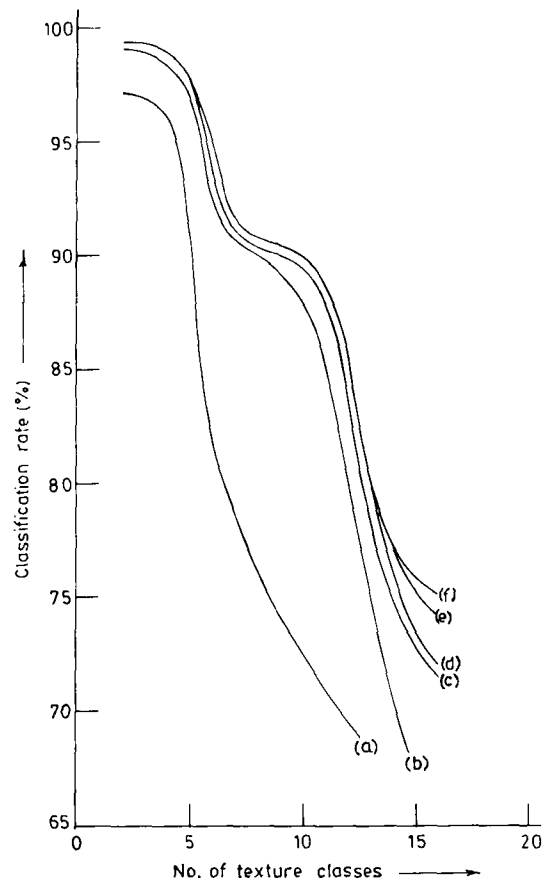


Figure 4. Classification rate of 100 test samples considering (a) 3 features f_1, f_2, f_3 , (b) 4 features f_1, f_2, f_3, f_4 , (c) 5 features f_1, f_2, f_3, f_4, f_5 , (d) 6 features $f_1, f_2, f_3, f_4, f_5, f_6$, (e) 7 features $f_1, f_2, f_3, f_4, f_5, f_6, f_7$, (f) 8 features $f_1, f_2, f_3, f_4, f_5, f_6, f_7, f_8$.

test samples. There is a sharp fall in classification rate when the number of classes increases from 2 to 6 and then the variation in classification rate is small when the number of classes varies from 7 to 10. Further increase in the number of classes results in sharp fall in classification rate. The reason for this curious stability of classification rate for 7–10 classes is not clear. However, it appears that if used for texture segmentation using fuzzy features, the most expected classification rate will correspond to this stable region ($\approx 90\%$).

Figure 4 shows the plots of the classification rate for a different number of features. It is seen that saturation occurs when the number of features is 6. We noted that f_7 and f_8 do not play a prominent role in texture classification if the other six features are present.

It is interesting to examine how fuzzy geometrical properties can be used for texture segmentation in a natural scene. The problem is being studied and useful results will be communicated in a future correspondence.

Acknowledgement

The authors wish to thank Prof. D. Dutta Majumder for his interest in the work and Prof. Anil Jain of Michigan State University for supplying the texture data.

References

- [1] Brodatz, P. (1966). *Texture: A Photographic Album for Artists and Designers*. Dover, New York.
- [2] Carlton, S.G. and O. Mitchell (1977). Image segmentation using texture and gray level. *Pattern Recognition and Image Processing Conf.*, Troy, NY, June 1977, 387–391.
- [3] Chaudhuri, B.B. (1991). Some shape definitions in fuzzy geometry of space. *Pattern Recognition Lett.* 12, 531–535.
- [4] Chaudhuri, B.B. (1992). Concave fuzzy sets: a concept complementary to the convex fuzzy set. *Pattern Recognition Lett.* 13, 103–106.
- [5] Chaudhuri, B.B. and B. Uma Shankar (1989). An efficient algorithm for extrema detection in digital images. *Pattern Recognition Lett.* 10, 81–85.
- [6] Chaudhuri, B.B. (1985). Membership evaluation. *Encyclopedia of Systems and Control*. Pergamon, Oxford, 1823–1825.
- [7] Haralick, R.M. (1979). Statistical and structural approach to texture. *Proc. IEEE* 67 (5), 786–804.
- [8] Ledley, R.S. (1972). Texture problems in biomedical pattern recognition. *Proc. 1972 IEEE Conf. on Decision and Control and 11th Symposium on Adaptive Processes*, New Orleans, LA, Dec. 1972.
- [9] Mitchell, O., C. Myers and W. Boyne (1976). A max-min measure for image texture analysis. *IEEE Trans. Comput.* 25, 725–736.
- [10] Prewitt, J.M.S. (1970). Object enhancement and extraction. In: B.S. Lipkin and A. Rosenfeld, Eds., *Picture Processing and Psychopictories*. Academic Press, New York, 75–149.
- [11] Rosenfeld, A. (1979). Fuzzy digital topology. *Information and Control* 40, 76–87.
- [12] Rosenfeld, A. (1984). The fuzzy geometry of image subsets. *Pattern Recognition Lett.* 2, 311–317.
- [13] Rosenfeld, A. and E. Troy (1970). Visual texture analysis. Tech. Rep. 70-116, Univ. of Maryland, College Park, MD, June 1970.
- [14] Rotolo, L.S. (1973). Automatic texture analysis for the diagnosis of pneumoconiosis. *26th ACEMB*, Minneapolis, MN, Sept. 30–Oct. 4, pp. 32.